CARBON 50 (2012) 4061–4067

Available at www.sciencedirect.com

SciVerse ScienceDirect

journal homepage: www.elsevier.com/locate/carbon

Highly responsive hydrogen gas sensing by partially reduced graphite oxide thin films at room temperature

Jianwei Wang [a], *Youngreal Kwak* [a], *In-yeal Lee* [a], *Sunglyul Maeng* [b], *Gil-Ho Kim* [a,*]

[a] *Samsung – SKKU Graphene Center, Sungkyunkwan Advanced Institute of Nanotechnology (SAINT) and School of Electronic and Electrical Engineering, Sungkyunkwan University, Suwon 440-746, Republic of Korea*

[b] *Department of Electronic and Electrical Engineering, Woosuk University, Wanju, Jeollabuk-do 565-701, Republic of Korea*

ARTICLE INFO

Article history:
Received 1 December 2011
Accepted 18 April 2012
Available online 24 April 2012

ABSTRACT

Novel chemo-resistive gas sensors based on reduced graphite oxide (rGO) thin films have been fabricated and evaluated for hydrogen detection. The rGO materials were thermally treated at various conditions and analyzed using X-ray diffraction, Fourier transform infrared spectroscopy, and X-ray photoelectron spectroscopy techniques to investigate the change of functional groups. The semiconductor type of the rGOs treated at different conditions were checked by flowing hydrogen gas at 20 cm^3/min (sccm) under 10 Torr partial pressure. The rGOs treated at 70 °C in atmosphere (rGO070a), 200 °C in a vacuum (rGO200v), and 500 °C in a vacuum (rGO500v) exhibited n-type, ambipolar, and p-type behavior, respectively. The rGO500v was adopted as active sensing element without any rare metal decoration, and its sensing response to hydrogen was studied by using air as carrier gas. The rGO500v exhibited good sensitivity (~4.5%), response time (~20 s), and recovery time (~10 s) to 160 ppm hydrogen gas at room temperature.

1. Introduction

Current issues involving global warming, air pollution, and the exhaustion of fossil fuels have drawn widespread and intense public attention. Hydrogen gas is expected to become the "common fuel of the future" because it is an efficient, clean, and renewable energy source. However, safety issues are one of the main challenges in the development of hydrogen energy. Hydrogen itself is colorless, odorless, and explosive. Hydrogen can be ignited easily with a very small amount of energy – as little as 0.02 mJ. The explosive range is wide, from 4% to 75%, and the hydrogen flame is invisible. To ensure safety, therefore, highly responsive and reliable sensors are needed to detect hydrogen leaks [1].

A variety of hydrogen sensors have been studied recently. Hydrogen sensors can be classified according to the four main types of detection mechanisms: chemo-resistive sensors, microelectronics-based sensors, surface acoustic wave sensors, and optical sensors. Among these, chemo-resistive sensors are most extensively employed owing to their relatively simple structure, cost-effective fabrication process, and well-established detection mechanism. Metal-oxide-semiconductors like SnO_2, ZnO, In_2O_3, and TiO_2 are the most favored gas sensing materials for chemo-resistive sensors. Metal oxide-based sensors normally operate at elevated temperatures that may cause high density hydrogen gas to ignite [2–5]. Since highly responsive hydrogen sensing based on metal oxide sensing materials is very difficult at low temperatures, coating or doping with a catalytic rare metal, such as platinum or palladium, is necessary. However, this may considerably increase the sensor production cost [6].

Consequently, sensing materials that enable low temperature operation of chemo-resistive hydrogen sensors without rare metal coating or doping have been sought by many

* *Corresponding author:* Fax: +82 031 299 4618.
E-mail address: ghkim@skku.edu (G.-H. Kim).

0008-6223/$ - see front matter
http://dx.doi.org/10.1016/j.carbon.2012.04.053

researchers. Single-walled carbon nanotubes (SWCNTs) were considered by many researchers as a candidate for this highly responsive room temperature hydrogen sensing material. Indeed, SWCNTs exhibited very high sensitivity to several oxidation gases at room temperature [7,8]. However, this material still needs rare metal decoration to achieve reasonable room temperature hydrogen sensing operation [9–11].

The important parameters of chemical sensors are sensitivity, response/recovery time, and 1/f noise level. Recently, it was reported that gas sensors made of a few layers of reduced graphite oxide (rGO) exhibit a 100-fold reduction of 1/f noise compared to SWCNT-based sensors [12]. Large amounts of ultra-thin graphite oxide (GO) can be easily produced by the chemical exfoliation of graphite through oxidation and subsequent dispersion in water. GO contains oxygen functional groups such as epoxide, carboxyl, and carboxylic acids. Owing to the disruption of the sp^2 bonded graphitic structure by the electronegative oxygen atoms in oxygen functional groups, GO is typically insulating. In order to lower the resistance of the material, reduction of GO through chemical, photo-catalytic, or thermal treatment is needed [13–16].

Gas sensors based on graphene and a few layers of rGO have been reported for NO_2 and NH_3 [17–20]. These sensors, however, exhibit very long response and recovery time. In the case of hydrogen gas sensors based on pristine rGO, poor sensitivity, response, and recovery were reported [21]. Thus, decoration of the rGO with platinum or palladium nanoparticles has been attempted by some researchers in the attempt to enhance the sensitivity of the hydrogen sensor [21–23]. Even though enhancement of sensitivity was achieved through the rare metal decoration, the poor response and poor recovery remained.

Though a single layer or a few layers of rGO may be ideal for highly sensitive gas sensor applications, ultra-thin multi-layer or periodically structured rGO may be preferred to reduce the cost of manufacturing the sensor. In this work, we introduce multi-layer rGO as a novel hydrogen sensor that exhibits high sensitivity and fast response and recovery behavior at room temperature.

2. Experimental details

GO was synthesized using the Hummers method, in which the natural graphite flakes 0.5 g and $NaNO_3$ 0.35 g were mixed and the H_2SO_4 30.7 g and $KMnO_4$ 1.95 g were added for the overnight reaction. Then, the reaction mixture was mixed with a diluted H_2SO_4 (5%) and H_2O_2 (30%) solution for further reaction. Finally, the compounds were rinsed by solution (3% H_2SO_4 and 0.5% H_2O_2) and DI water [24]. The obtained GO is composed of thin films with a thickness of several tens of nanometers.

The GO is then slightly reduced by thermal treatment at 70 °C in atmosphere (rGO070a), moderately reduced at 200 °C in a vacuum (rGO200v), or significantly reduced at 500 °C in a vacuum (rGO500v). The characteristics of rGOs were examined using X-ray diffraction (XRD), Fourier transform infrared (FT-IR) spectroscopy, and X-ray photoelectron spectroscopy (XPS).

For the gas sensing experiments, micro-hotplates were used. The micro-hotplates were composed of 150 μm–diameter integrated electronic devices (IEDs) and heaters of which the maximum temperature was 600 °C [25]. Fig. 1 shows an optical microscope image of the micro-hotplate device.

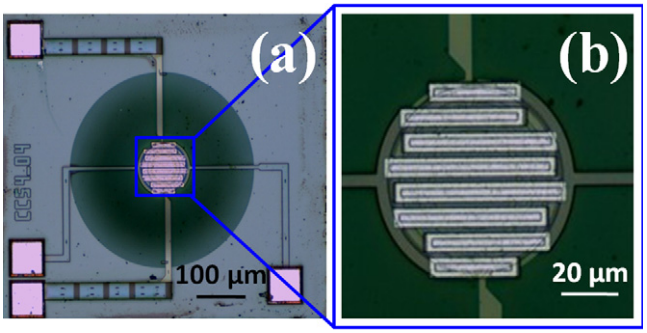

Fig. 1 – (a) Optical microscope image of the micro-hotplate device. (b) Magnification of the center of the micro-hotplate device.

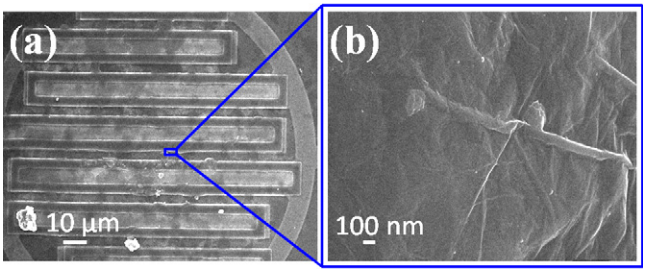

Fig. 2 – SEM image of rGO thin films deposited on IED at (a) ×800 magnification and (b) ×30000 magnification.

GO nanosheets 5 mg were first dispersed in DI water (10 ml), and a 0.1 μl solution was dropped onto the micro-hotplates to form an ultrathin GO network. The device was dried at room temperature and thermally treated at 70, 200, and 500 °C for 30 min to convert the GO into rGO. The patterns of the ultrathin GO network deposited onto the IED were investigated using scanning electron microscopy (SEM). Fig. 2 shows an SEM image of the rGO thin films deposited on the IED patterns of a micro-hotplate.

In order to check the semiconductor type of rGOs, the devices were loaded in the vacuum chamber and exposed to hydrogen gas of 20 cm^3/min (sccm) flow rate and 10 Torr partial pressure. During these experiments, the resistance of the devices was checked using the I–V measurement system for different micro-hotplate temperature conditions.

The sensing properties of devices were checked in the vacuum chamber by flowing hydrogen gas mixed with air. The concentrations of hydrogen gas were 30, 60, 100, and 160 ppm.

3. Results and discussion

Fig. 3 shows the XRD data of rGOs annealed for 30 min under various conditions. As shown in the figure, the (001) peak of the rGO070a is located at around 11.8°, corresponding to an interlayer distance of ~0.7 nm. The (001) peaks of rGO200v and rGO500v were observed at around 23.4° and 25.2°, respectively. The interlayer distances of rGO200v and rGO500v are

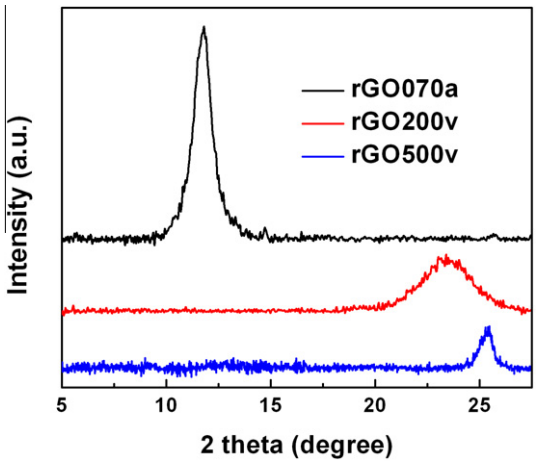

Fig. 3 – XRD data of rGOs thermally treated under various conditions.

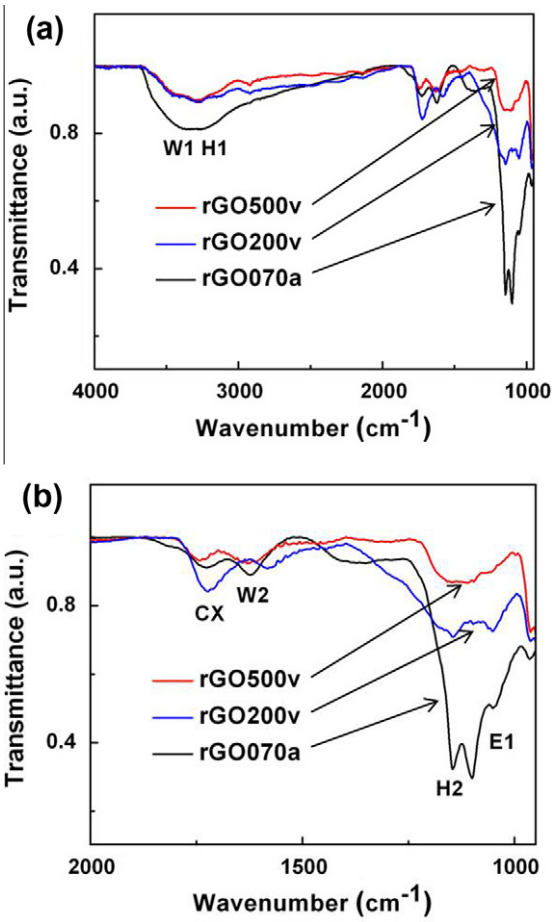

Fig. 4 – (a) FT-IR data of the rGO thin film under various conditions. (b) Magnification of the FT-IR data of the rGO thin film under various conditions.

approximately 0.4 and 0.35 nm. The (001) peak position of rGO tends to shift toward that of pristine graphite (26.2°) as the reduction temperature increases. The XRD data of rGO500v indicates the almost complete reduction of oxygen functional groups in the GO layers [26].

To determine which functional groups existed in the rGOs, FT-IR spectroscopy was performed. Fig. 4 presents FT-IR spectra of the rGOs. The rGO070a spectrum exhibit prominent hydroxyl peaks (H1 and H2 at 3442 and 1128 cm^{-1}) and water peaks (W1 and W2 at 3442 and 1625 cm^{-1}), with a small epoxide peak (E1 near 1070 cm^{-1}) and carboxyl peaks (CX near 1720 cm^{-1}).

The intensities of almost all the peaks shown in the FT-IR spectrum of rGO070a were significantly reduced in the FT-IR spectrum of rGO200v, except for the carboxyl peak (CX near 1720 cm^{-1}). In the FT-IR spectrum of rGO500v, the intensities of all peaks of functional groups were further reduced compared to those of rGO200v. This indicates that significant removal of functional groups took place.

XPS can be used to confirm chemical bonding between the functional groups and carbon atoms. Fig. 5 shows XPS C1s spectra of the rGOs and their deconvoluted peaks. The binding energy of 284.6 eV is attributed to the sp^2-hybridized carbon peak. The binding energies of 286.7–286.9, 288.3–288.6, and 289.7–290.4 eV can be attributed to peaks of hydroxyl, epoxide, and carboxyl functional groups, respectively [27–29].

The XPS C1s of rGO070a exhibits a slightly larger amount of hydroxyl groups thansp^2-hybridized carbon. The XPS C1s of rGO200v exhibits a slightly smaller amount of hydroxyl groups than does sp^2-hybridized carbon. For the XPS C1s of rGO500v, sp^2-hybridized carbon predominates among all functional groups. These data obtained from surface-sensitive XPS are consistent with the bulk-sensitive FT-IR results.

Fig. 6 shows the response of rGO070a to hydrogen gas exposure at room temperature. In this experiment, pure hydrogen gas was injected without carrier gas. As is indicated by the FT-IR and XPS data, rGO070a was not sufficiently reduced and exhibits very high resistance (~1 MΩ). This high resistance can be attributed to the wide band gap of slightly reduced GO. Thermally reduced pristine GO is known to be a p-type semiconductor [17–21]. If a p-type semiconductor is exposed to a reducing gas such as NH_3, CO, or H_2, an increase of resistance is expected.

Fig. 6 illustrates the decrease of resistance of rGO upon exposure to hydrogen gas. This indicates that the slightly reduced GO (rGO070a) is an n-type semiconductor. The hydrazine-hydrate reduced single layer GO and the multi-layer GO are known to exhibit excellent n-type behavior owing to the C–N bonding at the edge of graphene [30,31]. Jeong et al. reported n–p transition behavior of thermally reduced GO exposed to NO_2. They attributed this behavior to nitrogen doping [32]. This assumption is justified, as they reduced GO at a high temperature (600 °C) in the presence of a mixture of NH_3 and H_2. It is known that nitrogen doping occurs at temperatures as low as 300 °C when GO is annealed in the presence of NH_3 [33]. In the XPS spectra, the C–N peak is observed at 285.9 eV. The rGO070a was thermally reduced at temperatures as low as 70 °C in the presence of air; nitrogen doping may not cause the n-type behavior of the material, as the XPS C1s of rGO070a (Fig. 4a) does not exhibit a C–N peak.

Lu et al. reported that GO thermally reduced at temperatures as low as 200 °C in the presence of Ar exhibited n-type behavior [34]. Even though they attributed this to the unstead-

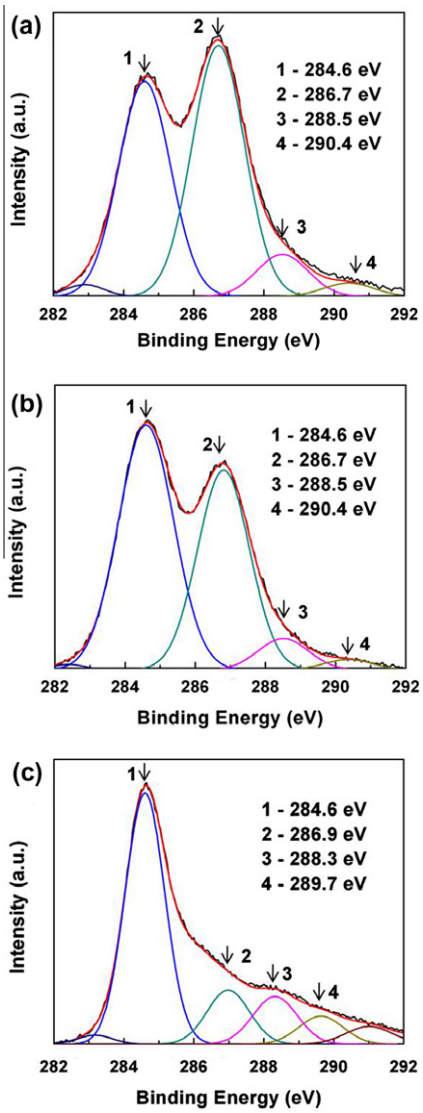

Fig. 5 – XPS C1s of (a) rGO070a, (b) rGO200v, and (c) rGO500v.The labels 1–4 denote peaks of sp^2-hybridized carbon, hydroxyl, epoxide, and carboxyl functional groups, respectively.

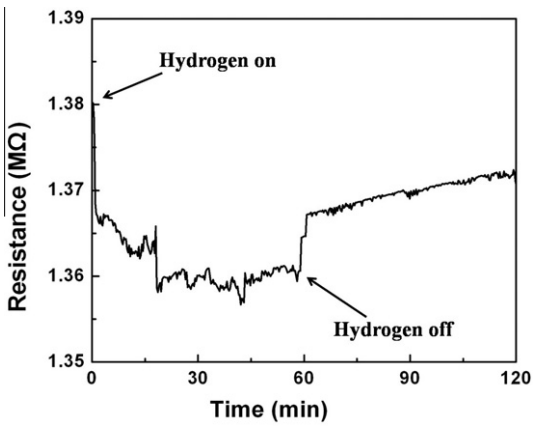

Fig. 6 – Resistance change of the rGO070a upon exposure to hydrogen gas at room.

iness of flow field in the chamber during the gas switching or some other accidental noise, our result clearly indicates that slightly reduced GO is n-type semiconductor. Fig. 6 shows that the response of the material is fairly fast while the recovery is extremely slow. As pristine graphene is known to bond weakly with hydrogen, this extremely slow recovery may be attributed to the strong bonding of hydrogen with active carbon atoms and to defect sites generated by the distortion of the graphene backbone by functional groups [35].

Fig. 7 shows the response of rGO200v to hydrogen gas exposure under various temperature conditions. This experiment was also implemented without using carrier gas to see the reduction effect solely by hydrogen. Considering that the baseline resistance is ~2 kΩ, it can be seen that the reduction occurred fairly successfully. The device exhibits very poor n-type characteristics at room temperature and moderate p-type characteristics at elevated temperatures. This indicates that rGO200v is an ambipolar semiconductor having both donor and acceptor levels in the energy band gap. This result is consistent with the observation made by Lu et al. [34]. The asymmetric nature of ambipolar behavior may be explained by assuming a shallow donor level with low density of states (DOS) and a deep acceptor level with high DOS. The

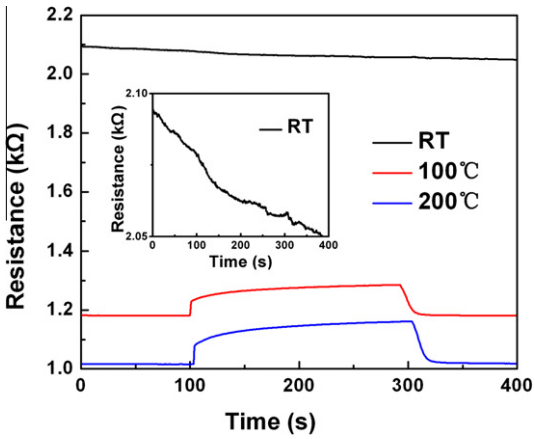

Fig. 7 – Resistance change of the rGO200v upon exposure to hydrogen gas under various temperature conditions.

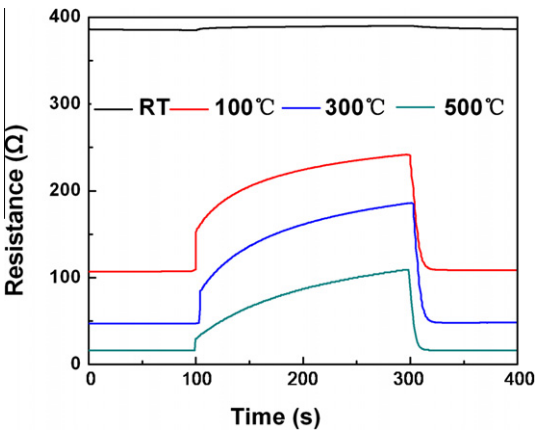

Fig. 8 – Resistance change of the rGO500v upon exposure to hydrogen gas under various temperature conditions.

sensing response of rGO200v to hydrogen at room temperature is negligible. The FT-IR and XPS data indicate that thermal treatment of GO at 200 °C in a vacuum reduces functional groups considerably. It is generally known that the elimination of sp^3-hybridized carbon bearing epoxide or hydroxyl functional groups enhances the sensitivity [14,19]. Since rGO070a contains significantly more functional groups than rGO200v, the considerably high sensitivity of rGO070a and the negligible sensitivity of rGO200v at room temperature cannot be explained simply by the above-mentioned hypothesis regarding rGO sensitivity. The change in functional group contents not only decreases the amount of sp^3-hybridized carbon but also influences the DOS in the band gap [36,37]. The experimental results indicate that the reduction of func-

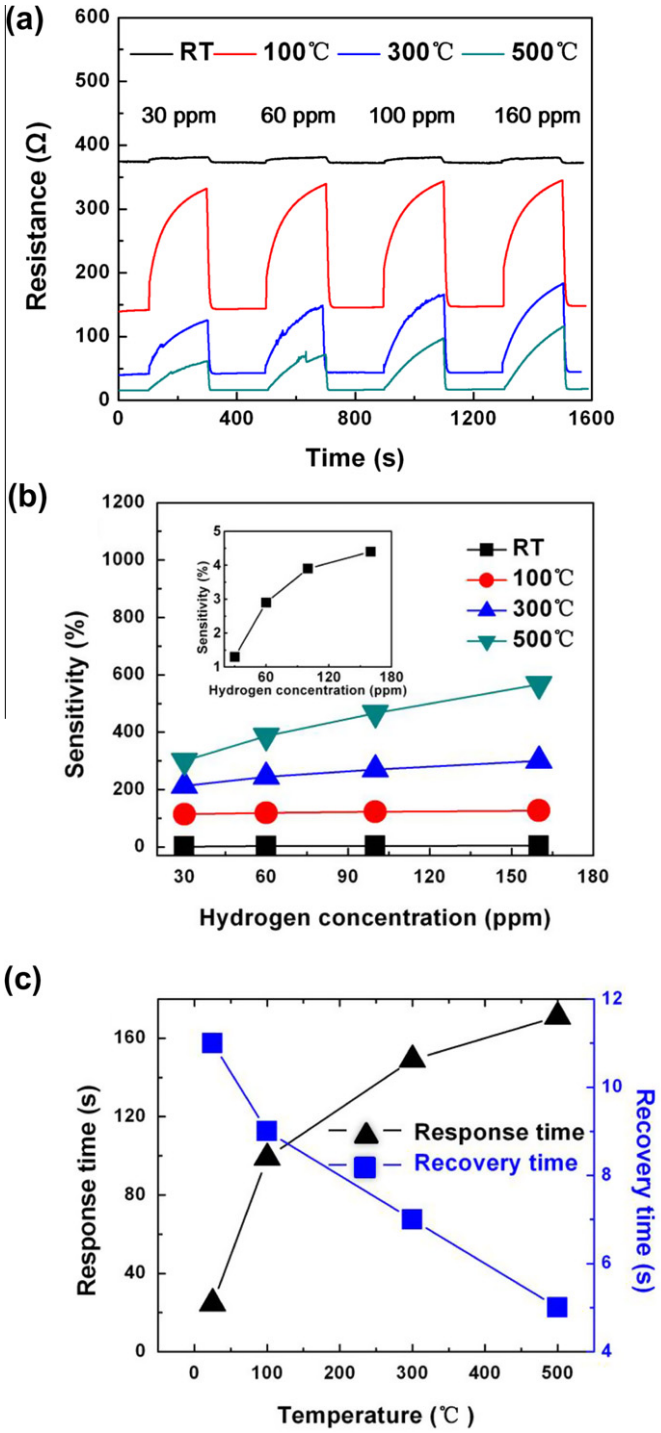

Fig. 9 – (a) Hydrogen gas sensing behavior of rGO500v at various gas concentrations and temperature conditions. (b) The dependence of sensitivity on the gas concentration. (c) Temperature dependence of response and recovery time of rGO500v exposed to 160 ppm hydrogen gas.

tional groups at 200 °C in a vacuum leads to a decrease in the DOS of the shallow donor level of rGO, which dominantly contributes to the conduction at room temperature.

Fig. 8 shows the increase of resistance of rGO upon exposure to hydrogen gas for all temperature conditions. This indicates that the shallow donor levels no longer exist and the heavily reduced GO (rGO500v) is p-type semiconductor. The very low resistance at room temperature (~300 Ω) indicates that the material was significantly reduced, and this agrees well with FT-IR and XPS data. This means that the band gap of the material is very small.

The sensitivity of a p-type semiconducting gas sensor, S (%), is generally defined as $[(R_o - R_g)/R_o] \times 100$, where R_o represents the baseline resistance and R_g represents the resistance of the device exposed togas. The response time of the gas sensor T_{res} can be defined as the time needed for its resistance to change from its initial value to 90% of its highest value. The recovery time of the gas sensor T_{rec} can be defined as the time taken for its resistance to be reduced by 90% from its highest value. The hydrogen gas sensing characteristics of rGO500v were checked using 1 atm air as carrier gas for different gas concentration and substrate temperatures as shown in Fig. 9a.

Fig. 9b shows the dependence of sensitivity on the gas concentration; the sensitivity is calculated from the sensing behavior shown in Fig. 9a. The sensitivity tends to increase as the hydrogen concentration increases. Fig. 9b also demonstrates that our rGO-based hydrogen sensor exhibits high sensitivity without any raremetal decoration. This high sensitivity may be attributed to highly active carbon sites on the surface of the rGO500v generated by distortions of the graphene backbone caused by remaining functional groups [13,26].

Fig. 9c shows the dependence of the response and recovery time of device on the operation temperature when the hydrogen concentration was fixed at 160 ppm. Here, the room temperature results are remarkable. The response time and the recovery time are ~20 and ~10 s, respectively. Other researchers reported very slow response time and recovery time (10^3~10^5 s) for rGO-based hydrogen sensors, even with decoration by raremetal nanoparticles [21–23].

In regards to the point of sensitivity, sensor operation at 500 °C is preferable. However, high temperature operation of hydrogen sensors is problematic in regards to both economy and safety; overall, room temperature operation is highly desirable. The fairly good sensitivity (~4.5%) and excellent response time (~20 s) and recovery time (~10 s) of rGO500v to 160 ppm hydrogen at room temperature are adequate for high-end industrial applications.

4. Conclusions

Graphite oxide (GO) thin films were partially reduced under different thermal environments. The effect of heat treatment temperature on reduction of the functional groups of the GO thin film was studied using XRD, FT-IR, and XPS analyses. Even though the functional groups in rGO500v were considerably decreased compared to those in rGO070a and rGO200v, they were not negligible. The semiconductor types of rGOs treated at different thermal process were studied by exposing hydrogen gas to the devices loaded in a vacuum chamber. rGO070a exhibited a considerable decrease of resistance at room temperature upon exposure to the hydrogen gas; this indicates that rGO070a is an n-type semiconductor. rGO200v exhibited a very small decrease of resistance at room temperature and a moderate increase of resistance at elevated temperatures upon exposure to hydrogen gas; this indicates that rGO200v is an asymmetric ambipolar semiconductor. rGO500v exhibited a considerable increase of resistance at all temperatures upon exposure to hydrogen gas; this indicates that rGO500v is a p-type semiconductor. These results indicate that the reducing temperature affects the distribution of DOS in the band gap as well as the band gap size. rGO500v was tested as hydrogen gas sensor by using 1 atm air as carrier gas. The device was proved to function as an effective hydrogen sensor at room temperature, with moderate sensitivity and excellent response and recovery behavior.

Acknowledgements

This research was supported by World Class University program funded by the Ministry of Education, Science and Technology through the National Research Foundation of Korea (R32-10204).

REFERENCES

[1] Pritchard DK, Royle M, Willoughby D. Installation permitting guidance for hydrogen and fuel cell stationary applications. Health and Safety Laboratory UK, RR715. 2009.
[2] Kenji W, Makoto E. Hydrogen sensing properties of SnO_2 subjected to surface chemical modification with ethoxysilanes. Sens Actuators B 2000;62(3):211–9.
[3] Park SJ, Park J, Lee HY, Moon SE, Park KH, Kim J, et al. High sensitive NO_2 gas sensor with low power consumption using selectively grown ZnO nanorods. J Nanosci Nanotechnol 2010;10(5):3385–8.
[4] Moon SE, Lee HY, Lee JW, Choi NJ, Park SJ, Kwak JH, et al. Low power consumption and high sensitivity carbon monoxide gas sensor using indium oxide nanowire. J Nanosci Nanotechnol 2010;10(5):3189–92.
[5] Miyazaki H, Hyodo T, Shimizu Y, Egashira M. Hydrogen-sensing properties of anodically oxidized TiO_2 film sensors: effects of preparation and pretreatment conditions. Sens Actuators B 2000;108(1–2):457–72.
[6] Tien LC, Sadik PW, Norton DP, Voss LF, Pearton SJ, Wang HT, et al. Hydrogen sensing at room temperature with Pt-coated ZnO thin films and nanorods. Appl Phys Lett 2005;87:222105.
[7] Li J, Lu YJ, Ye Q, Cinke M, Han J, Meyyappan M. Carbon nanotube sensors for gas and organic vapor detection. Nano Lett 2003;3:929–33.
[8] Maeng S, Moon S, Kim S, Lee H, Park S, Kwak J, et al. Highly-sensitive NO_2 sensor arrays based on undecorated single-walled carbon nanotube monolayer junctions. Appl Phys Lett 2008;93(11):113111.
[9] Mubeen S, Zhang T, Yoo B, Deshusses MA, Myung NV. Palladium nanoparticles decorated single-walled carbon nanotube hydrogen sensor. J Phys Chem C 2007;111(17):6321–7.
[10] Sun Y, Wang HH. Electrodeposition of Pd nanoparticles on single-walled carbon nanotubes for flexible hydrogen sensors. Appl Phys Lett 2007;90:213107.

[11] Sayagoa I, Terradob E, Aleixandrea M, Horrilloa MC, Fernándeza MJ, Lozanoa J, et al. Novel selective sensors based on carbon nanotube films for hydrogen detection. Sens Actuators B 2007;112(1):75–80.
[12] Robinson JT, Perkins FK, Snow ES, Wei Z, Sheehan PE. Reduced graphene oxide molecular sensors. Nano Lett 2008;8(10):3137–40.
[13] Stankovich S, Piner RD, Chen X, Wu N, Nguyen ST, Ruoff RS. Stable aqueous dispersions of graphitic nanoplatelets via the reduction of exfoliated graphite oxide in the presence of poly(sodium 4-styrenesulfonate). J Mater Chem 2006;16:155–8.
[14] Williams G, Seger B, Kamat PV. TiO_2–graphene nano composites UV-assisted photo catalytic reduction of graphene oxide. ACS Nano 2008;2(7):1487–91.
[15] Jung I, Dikin DA, Piner RD, Ruoff RS. Tunable electrical conductivity of individual graphene oxide sheets reduced at "low" temperatures. Nano Lett 2008;8(12):4283–7.
[16] Wang X, Zhi L, Mullen K. Transparent, conductive graphene electrodes for dye-sensitized solar cells. Nano Lett 2008;8(2):323–7.
[17] Schedin F, Geim AK, Morozov SV, Hill EW, Blake P. Detection of individual gas molecules adsorbed on graphene. Nat Mater 2007;6:652–5.
[18] Lu G, Ocola LE, Chen JH. Gas detection using low-temperature reduced grapheme oxide sheets. Appl Phys Lett 2009;94:08311.
[19] Fowler JD, Allen MJ, Tung VC, Yang Y, Kaner RB, Weiller BH. Practical chemical sensors from chemically derived graphene. ACS Nano 2009;3(2):301–6.
[20] Han TH, Huang YK, Tan ATL, Dravid VP, Huan J. Steam etched porous grapheme oxide network for chemical sensing. J Am Chem Soc 2011;133:15264–7.
[21] Chu BH, Nicolosi J, Lo CF, Strupinski W, Pearton SJ, Ren F. Effect of coated platinum thickness on hydrogen detection sensitivity of graphene-based sensors. Electrochem Solid State Lett 2011;14:K43–5.
[22] Lange U, Hirscha T, Mirskyb VM, Wolfbeisa OS. Hydrogen sensor based on a graphene–palladium nanocomposite. Electrochim Acta 2011;56(10):3707–12.
[23] Kaniyoor A, Jafri RI, Arockiadoss T, Ramaprabhu S. Nanostructured Pt decorated graphene and multi walled carbon nanotube based room temperature hydrogen gas sensor. Nanoscale 2009;1:382–6.
[24] Hirata M, Gotou T, Horiuchi S, Fujiwara M, Ohba M. Thin-film particles of graphite oxide: high-yield synthesis and flexibility of the particles. Carbon 2004;42(14):2929–37.
[25] Maeng S, Guha P, Udrea F, Ali Z, Santra S, Gardner J, et al. SOI CMOS-based smart gas sensor system for ubiquitous sensor networks. ETRI J 2008;30:516–25.
[26] Gomez-Navarro C, Weitz RT, Bittner AM, Scolari M, Mews A, Burghard M, et al. Electronic transport properties of individual chemically reduced graphene oxide sheets. Nano Lett 2007;7(11):3499–503.
[27] Yumitori S. Correlation of C1s chemical state intensities with the O1s intensity in the XPS analysis of anodically oxidized glass-like carbon samples. J Mater Sci 2000;35:139–46.
[28] Yang D, Velamakanni A, Bozoklu G, Park S, Stoller M, Piner RD, et al. Chemical analysis of graphene oxide films after heat and chemical treatments by X-ray photoelectron and Micro-Raman spectroscopy. Carbon 2009;47(1):145–52.
[29] Jeong HK, Colakerol L, Jin MH, Glans PA, Smith KE, Lee YH. Unoccupied electronic states in graphite oxides. Chem Phys Lett 2008;460:499–502.
[30] Tung VC, Allen MJ, Yang Y, Kaner RB. High-throughput solution processing of large-scale graphene. Nat Nanotechnol 2009;4:25–9.
[31] Late DJ, Ghosh A, Subrahmanyam KS, Panchakarla LS, Krupanidhi SB, Rao CNR. Characteristics of field-effect transistors based on undoped and B-and N-doped few-layer graphenes. Solid State Commun 2010;150:734–8.
[32] Jeong HY, Lee DS, Choi HK, Lee DH, Kim JE, Lee JY, et al. Flexible room-temperature NO_2 gas sensors based on carbon nanotubes/reduced graphene hybrid films. Appl Phys Lett 2010;96:213105.
[33] Li X, Wang H, Robinson JT, Sanchez H, Diankov G, Dai H. Simultaneous nitrogen doping and reduction of graphene oxide. J Am Chem Soc 2009;131(43):15939–44.
[34] Lu G, Ocola LE, Chen JH. Reduced graphene oxide for room-temperature gas sensors. Nanotechnology 2009;20:445502.
[35] Zhang YH, Chen YB, Zhou KG, Liu CH, Zeng J, Zhang HL, et al. Improving gas sensing properties of graphene by introducing dopants and defects: a first-principles study. Nanotechnology 2009;20:185504.
[36] Boukhvalov DW, Katsnelson MI. Modelling of graphite oxide. J Am Chem Soc 2008;130:10697–701.
[37] Xu Z, Xue K. Engineering graphene by oxidation: a first-principles study. Nanotechnology 2010;21:045704.